AGU PUBLICATIONS

Geophysical Research Letters

RESEARCH LETTER
10.1002/2015GL064488

Key Points:
- Annual mean wave power is very variable, particularly in the North Atlantic
- Good correlation between wave power and climate indices (NAO)
- Reconstructed wave climate since 1665 shows high variability over all timescales

Supporting Information:
- Supporting Information S1

Correspondence to:
H. Santo,
harrif.santo@eng.ox.ac.uk

Citation:
Santo, H., P. H. Taylor, T. Woollings, and S. Poulson (2015), Decadal wave power variability in the North-East Atlantic and North Sea, *Geophys. Res. Lett.*, *42*, 4956–4963, doi:10.1002/2015GL064488.

Received 7 MAY 2015
Accepted 21 MAY 2015
Accepted article online 1 JUN 2015
Published online 30 JUN 2015

Decadal wave power variability in the North-East Atlantic and North Sea

H. Santo[1], P. H. Taylor[1], T. Woollings[2], and S. Poulson[1]

[1]Department of Engineering Science, University of Oxford, Oxford, UK, [2]Department of Physics, Atmospheric, Oceanic and Planetary Physics, University of Oxford, Oxford, UK

Abstract Estimation of the long-term behavior of wave climate is crucial for harnessing wave energy in a cost-effective way. Previous studies have linked wave heights to the north-south atmospheric pressure anomalies in the North Atlantic, suggesting that the wave climate fluctuates as a response to changes in zonal circulation in the atmosphere. We identify changes in wave power in the North-East Atlantic that are strongly correlated to the dominant pressure anomalies, the North Atlantic Oscillation (NAO), and other modes. We present a reconstructed wave power climate for 1665–2005, using a combination of known and proxy indices for the NAO and other modes. Our reconstruction shows high interannual and multidecadal variability, which makes wave energy prediction challenging. This variability should be considered in any long-term reliability analysis for wave energy devices and in power scheme economics.

1. Introduction

The variability of the wave energy resource in the open ocean is large and spans multiple time scales. This limits our ability to predict accurately the future resource and yield from wave energy schemes. Apparent upward trends in wave heights were reported over more than a decade ago in the North Atlantic [*Carter and Draper*, 1988; *Bacon and Carter*, 1991; *Kushnir et al.*, 1997] and in the North Pacific [*Allan and Komar*, 2000]. Trends in ocean surface winds and wave heights [*Young et al.*, 2011, 2012; *Zieger et al.*, 2014] as well as rain [*Wentz et al.*, 2007] have also been investigated recently for global coverage. These trends have been estimated for relatively short periods and do not always reflect long-term behaviors. Nevertheless, such an upward trend is clearly of interest for wave energy production but also has created concern when linked to global warming. To understand how the wave climate fits into the Earth system, previous studies have been conducted by establishing relationships between wave parameters and atmospheric pressure gradients. The highest correlations are found in the North-East Atlantic [see, for example, *Bacon and Carter*, 1993; *Woolf et al.*, 2002; *Shimura et al.*, 2013], which suggest there is an interplay between the wave climate and the atmosphere, at least in that region.

Here we evaluate the relationship of the wave power climate from hindcast data (wave model driven by carefully reconstructed weather information) to the sea level pressure anomalies in the North Atlantic and North Sea, the North Atlantic Oscillation (NAO), and other modes, by constructing a wave power predictor model based on standard linear regression. *Mackay et al.* [2010], *Neill and Hashemi* [2013], and *Neill et al.* [2014] conducted similar studies by looking at correlation of wave power variability with the NAO at different locations, all with hindcast data, and obtained a positive correlation. What is different in our study is that we incorporate other teleconnection patterns, introduce the use of proxy indices, and infer back to seventeenth century the historic wave climate at multiple locations around the North-East Atlantic and North Sea to reveal a long-term perspective.

2. Data and Methods

We have wave data at three locations in the North-East Atlantic and the northern North Sea. Figure 1a shows the locations: Schiehallion (60.30°N, 04.00°W), Haltenbanken (65.36°N, 07.14°E), and Forties (57.79°N, 00.88°E). The wave data are a combination of measured buoy (for Haltenbanken from 1980 to 2001 and Forties from 1974 to 1997) and hindcast data (for all three locations from 1958 to 2011). The hindcast data we used are the Norwegian 10 km Reanalysis Archive (NORA10) developed by the Norwegian Meteorological Institute [*Reistad et al.*, 2011]. It is a regional High-Resolution Limited Area Model (atmospheric model) [*Unden et al.*, 2002] and WAM Cycle-4 (wave model) [*Group*, 1988] hindcast covering northeastern North

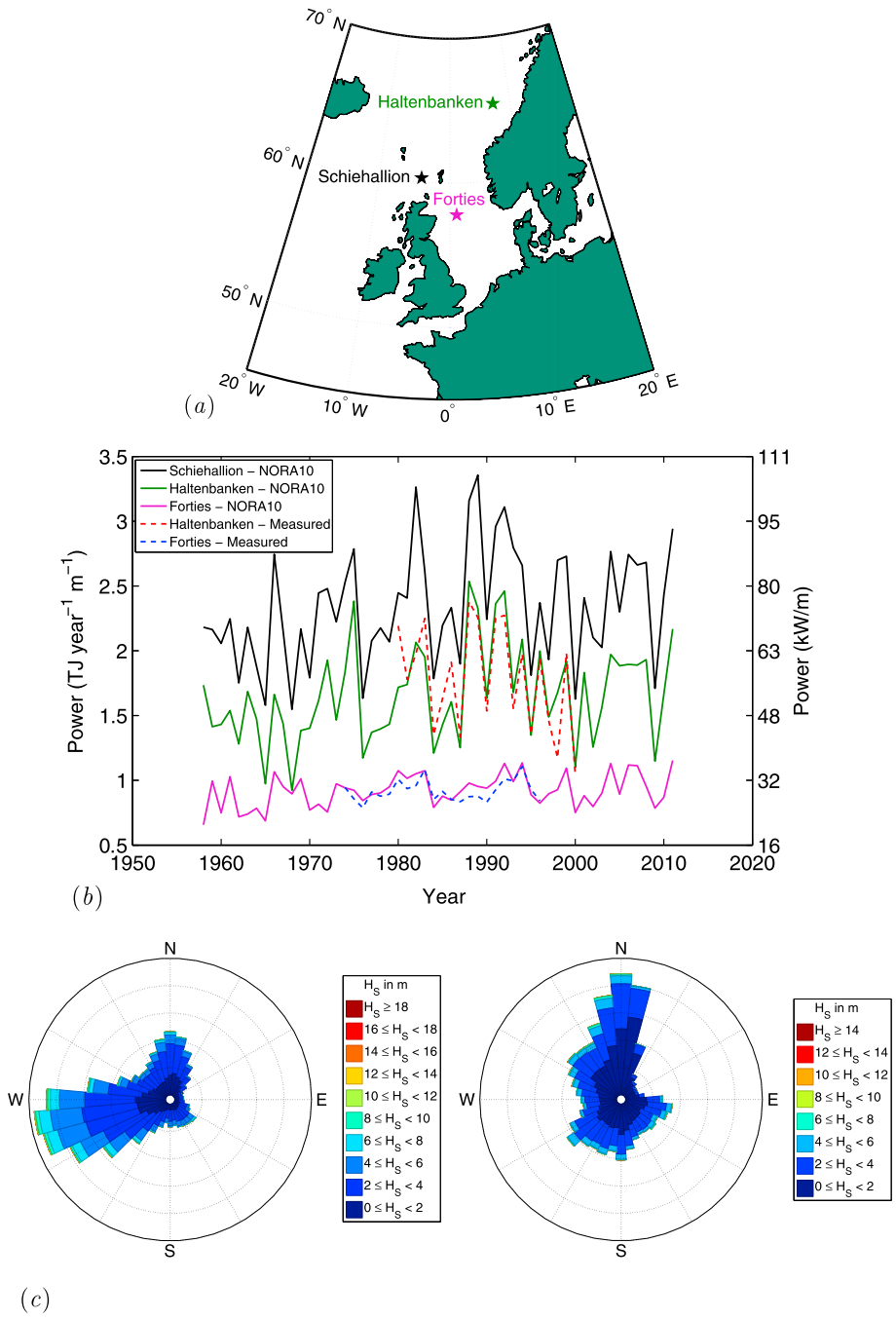

Figure 1. Geographic and wave information of the three locations of the wave data. (a) Map of the three locations: Schiehallion, Haltenbanken, and Forties. (b) Available mean wave power resources at three locations from measured and hindcast data. (c) Wave height rose distributions for Schiehallion and Forties.

Atlantic. The regional model uses wind and wave boundary conditions (dynamic downscaling to a spatial resolution of 10–11 km) from the European Centre for Medium-Range Weather Forecasts ERA-40 reanalysis (1958–2002) [*Uppala et al.*, 2005] and is extended using the ERA-Interim reanalysis from 2002 to 2011. The moving boundary of sea ice is included in the model.

The wave data available in 3 h intervals contain information such as date, time, significant wave height (H_s), peak spectral wave period (T_p), mean wave period (T_m or T_{m01}, only in hindcast data), zero-crossing period (T_z or T_{m02}, only in measured data), wind speed, wind, and wave directions. The measured data of Haltenbanken and Forties contain some gaps in T_p; however, the measured H_s time history is complete

(see Table S1 in the supporting information). Treating the data set as a single block, we use the correlation between H_s and T_p to provide an appropriate T_p estimate when required, in order to form a complete measured H_s and T_p time history required for wave power calculation. This patching was performed in several different ways; this made no difference to the subsequent results (see Figure S1 in the supporting information). The measured data of Forties also contain some gaps in both H_s and T_p (12% of the total data). The missing H_s values were patched with the hindcast H_s values as the measured H_s record agrees reasonably well with the hindcast H_s record (see Figures S2 and S3 in the supporting information). The missing T_p values were then filled by the method described previously. Normalized root-mean-squared error is used to quantify model/buoys comparisons: the T_p comparisons for Haltenbanken and Forties are 21% and 20%, respectively, and the H_s comparisons are 24% and 17%, respectively, over the period of available measurements. All the hindcast data are continuous.

The instantaneous wave power per unit length of wavefront is defined as

$$P = \frac{\rho g^2}{64\pi} H_s^2 T_p$$

where H_s is the significant wave height, T_p is the peak spectral wave period, ρ is the water density, and g is the gravitational acceleration. Strictly speaking, the wave power should be calculated using the energy period (T_e), which is likely to be midway between T_p and T_m [*Tucker and Pitt*, 2001]. However, as the available period from both the hindcast and measured data is T_p rather than T_e or T_m, T_p was used instead so that a comparison of wave power based on hindcast and measured data is possible. We have investigated the impact of using T_p versus T_m and find that the fluctuation from year to year for wave power is essentially unaltered by the use of T_p or T_m, and we would expect likewise for T_e (see Figures S4 and S5 in the supporting information). The total energy available over a year was obtained by numerical integration of the 3-hourly wave power values over that particular year, this can also be interpreted as the average wave power per meter of wavefront for that year (expressed in TJ/yr/m). It is common in the renewable energy field to express the average power in terms of TJ/year, but this could equally be expressed in kW (1 TJ/yr/m = 31.69 kW/m). The average year-by-year power was obtained by splitting the years summer to summer (the middle of July 1 year to the middle of July the subsequent year, taking the year date from the part of record up to December) from the continuous wave power time history record, thus avoiding splitting winters when the most energy is available.

Figure 1b shows the available average annual wave power for each location. The wave power resources at Haltenbanken and Forties derived from both measured and hindcast data are similar (R^2 = 0.76 and 0.70, respectively) which supports the accuracy of the hindcast model. As the hindcast data contain a longer period of available information (over 40 years), the hindcast data are used subsequently for the analysis to allow more statistically significant conclusions to be drawn.

Interestingly, from the same figure, there is considerable variability on a year-by-year basis and over decades long. The largest short-term variation occurs in two consecutive years immediately after 1980 for the Schiehallion data, with a variation of almost a factor of 2. Schiehallion and Haltenbanken seem to be strongly correlated, with similar short-term and long-term variability despite the large distance between these two locations, but Forties is different as it is more sheltered by land surrounding the North Sea. This becomes clearer when looking at the wave rose distributions of H_s against incoming wave direction as shown in Figure 1c for Schiehallion and Forties, respectively, color coded with the number of occurrences of H_s. From the wave rose distributions of both Schiehallion and Haltenbanken (not shown), the dominant waves are from the west generated by storms in the open North Atlantic. These waves are effectively shielded from propagating into the North Sea, so at Forties on average the larger waves are from the north, presumably originating from storms heading toward northern Scandinavia. However, there is a significant second contribution from waves from the southeast. It will be shown that this split of the wave rose into two main wave directions leads to a reduced wave power variability compared to that of points in the open North Atlantic. This variability can be quantified as coefficient of variation (CV = ratio of the standard deviation to the mean). The CVs for Schiehallion and Haltenbanken are 19% and 21%, while for Forties is 14%. In order to yield optimum output from wave energy production, this large variability in the available wave power needs to be taken into consideration. But what drives this variability?

3. Temporal and Spatial Wave Climate Variability

A primary agent of the large variability observed in the wave power in this North Atlantic region is the North Atlantic Oscillation (NAO), the dominant recurring and persistent large-scale pattern of pressure anomalies.

The NAO measures variation in the Atlantic eddy-driven jet which controls the near-surface westerly winds [*Woollings et al.*, 2010], so a link between pressure anomalies and wave power seems likely. The NAO has long been known to affect climate variability in the Northern Hemisphere, particularly in the winter months [see, for example, *Hurrell*, 1995; *Hurrell and Van Loon*, 1997; *Hurrell et al.*, 2003].

Several indices have been proposed to characterize the spatial pattern of the NAO. We use monthly teleconnection indices tabulated by National Oceanic and Atmospheric Administration (NOAA) Climate Prediction Center (www.cpc.ncep.noaa.gov) which is based on the rotated empirical orthogonal function (EOF) analysis calculated by *Barnston and Livezey* [1987] and discussed further in *Moore et al.* [2013]. In the North Atlantic region, the first EOF mode is referred to as the NAO, while the second and third modes are referred to as the East Atlantic pattern (EA) and the Scandinavian pattern (SCA), respectively. These three EOF modes will be correlated with the available wave resources. The available indices date from January 1950 to the present. However, in order to infer the wave climate back to the past to produce a long enough wave climate record, we will introduce a set of proxy indices.

We correlated the wave power with a winter average of the teleconnection indices rather than an annual average, as the year-to-year variability observed in the available wave power is more likely to be driven by the energy available in the winter. Each winter average was obtained by averaging 6 month values of monthly teleconnection indices centered around the middle of January (i.e., from mid-October to mid-April). In formulating a predictor model to establish relationships between the wave power and the teleconnections, the long timescale variations in the EA and the SCA were removed because both of them are correlated with the NAO ($R^2 \sim 0.7$ for a 10 year moving average, see Figures S6 and S7 in the supporting information) over the period of interest (from 1950 to 2013). Hence, we imposed a low-pass filter to the NAO index (moving average) and a high-pass filter to both the EA and the SCA indices. We formulated a predictor model $P_{\text{predictor}}$ for wave power based on variance minimization and standard linear regression, shown as

$$f = \frac{1}{\sum (P(t) - \overline{P})^2} \times \sum [(P(t) - \overline{P}) - \tilde{b}(\mathrm{EA}_{hi}(t) - \overline{\mathrm{EA}}) - \tilde{c}(\mathrm{NAO}(t) - \overline{\mathrm{NAO}}) - \tilde{d}(\mathrm{SCA}_{\mathrm{hi}}(t) - \overline{\mathrm{SCA}})]^2$$

$$P_{\text{predictor}} = \overline{P} \times [1 + b(\mathrm{EA}_{\mathrm{hi}}(t) - \overline{\mathrm{EA}}) + c(\mathrm{NAO}(t) - \overline{\mathrm{NAO}}) + d(\mathrm{SCA}_{\mathrm{hi}}(t) - \overline{\mathrm{SCA}})]$$

where f is the variance to be minimized, $P(t)$ is the annual wave power signal, $\overline{P}$ is the average power over the period of available data, $\mathrm{NAO}(t)$ is the moving average of the NAO index, $\overline{\mathrm{NAO}}$ is the mean of the NAO moving average, $\mathrm{EA}_{\mathrm{hi}}(t)$ and $\mathrm{SCA}_{\mathrm{hi}}(t)$ are the high-pass filtered EA and SCA signals, while $\overline{\mathrm{EA}}$ and $\overline{\mathrm{SCA}}$ are the mean of the $\mathrm{EA}_{\mathrm{hi}}(t)$ and $\mathrm{SCA}_{\mathrm{hi}}(t)$ signals, respectively. Constants resulting from the variance minimization are $\tilde{b}$, $\tilde{c}$, and $\tilde{d}$, while $c = \tilde{c}/\overline{P}$ and likewise b and d are nondimensionalized constants, which reflect the relative importance of the EA, the NAO, and the SCA signals in predicting wave power, respectively (see Table S2 in the supporting information). The individual cutoff values of the low-pass and high-pass filters are chosen to minimize the variance in each case. After minimization, we obtain a combination of a window length of 1 year for the NAO moving average; i.e., we are fitting the model with the unaltered NAO signal, and a high-pass filter length of 11 years or longer for the EA and the SCA. Hence, in our predictor model the NAO describes variability in all time scales, while both the EA and the SCA account for short-term fluctuations only.

We obtain strong correlations between the available wave power and the predictor model for both Haltenbanken and Schiehallion ($R^2 > 0.7$), but weaker correlation for Forties ($R^2 = 0.41$), as shown in Figure 2a. Strong correlation for Haltenbanken and Schiehallion suggests that the variability in wave power in the open North Atlantic is strongly associated with the NAO, which is related to the occurrence of the westerly swells moving toward northern Europe. At least for the open North Atlantic, the future predictability of the wave power is largely dependent on the predictability of the future behavior of the NAO and other modes, as also suggested by *Woolf et al.* [2002].

Various tests have been conducted to test the robustness of the correlation analysis. The residual of each linear regression is close to normally distributed and shows no significant autocorrelation structure. Testing for overfitting was performed by randomly reordering the EA signal 5000 times and correlating the model

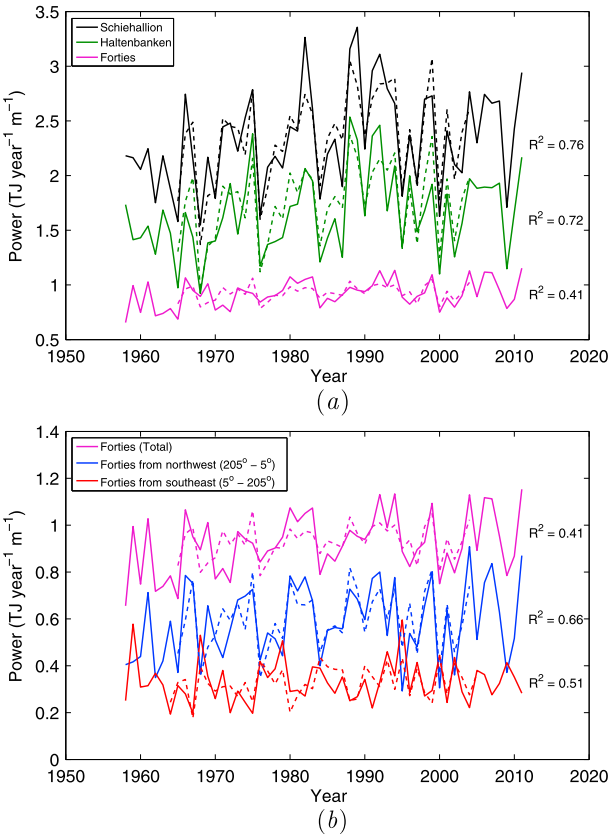

Figure 2. Comparison of the actual (solid lines) and predicted (dashed lines) wave power. (a) For the three locations. (b) For Forties with angle partitioning.

containing the reordered EA and known SCA and NAO signals with the hindcast wave power to obtain histogram of R^2 coefficients. The EA signal was chosen for this because it is the weakest contributor. In general, the R^2 coefficient is in the 98th percentile suggesting the inclusion of the EA signal was making a genuine improvement to the model. Trend analysis was conducted by removing a linear in time component from the wave power, and this made little difference, suggesting the correlation is robust (see Figures S8–S11 in the supporting information).

To further investigate why the correlation works less well for Forties in the North Sea, the total available wave power was partitioned based on the incoming wave direction: waves coming from northwest (205°–5°) and southeast (5°–205°), where 0° is pointing to the north and 90° to the east. From the wave rose distribution at Forties shown in Figure 1c, the chosen range of partition splits the total wave power into two components of comparable magnitude. The range of the partitioned angle is chosen to give maximum correlation with the NAO and other modes. The angle partitioning method produces a pair of wave power signals that are in antiphase with each other, being associated with the positive or negative phases of the NAO and other modes, as shown in Figure 2b. When the NAO is in its positive phase (or less negative), the northerly waves in Forties are more dominant than the southerly waves (peaks for the northwest signal and nadirs for the southeast signal), and the situation is reversed when the NAO is in its negative phase (or less positive). Better correlation for each of the pair of the antiphase signals with the predictor model is obtained (R^2 = 0.5–0.6). However, since both the antiphase signals are of comparable magnitude with some degree of variability (CV = 28% for both), the total wave power signal at Forties has weaker correlation with our linear predictor model and also reduced variability (CV = 14%). Thus, on the component basis Forties is also influenced by the variability of the NAO much like the locations in the open North Atlantic, but the net overall effect is considerably smaller. In support of findings from *Neill and Hashemi* [2013], the North Sea could potentially provide a better location for wave power production if higher reliability is required. A nonlinear predictor model incorporating positive and negative phases of the NAO and other modes, for example, in *Cassou et al.* [2011], might improve the correlation for Forties.

4. Reconstruction of Wave Power Climate

None of the available wave data or teleconnection indices are long enough to produce a long-term representation of the historic wave climate, which is the interest of this study. Hence, proxy indices are introduced using the historical reconstructed monthly 500 mbar pressure maps computed by *Luterbacher et al.* [2002] from 1659 to 1998. Instead of performing a full EOF analysis on the pressure maps back to the past to produce the three atmospheric modes, we introduce a simpler method to obtain each proxy index. The pressure maps of *Luterbacher et al.* [2002] were regressed with the three known indices of the NAO from the Climate Prediction Center (CPC) over the period of 1950–1998. Figure 3 (left column) shows the spatial correlation of the

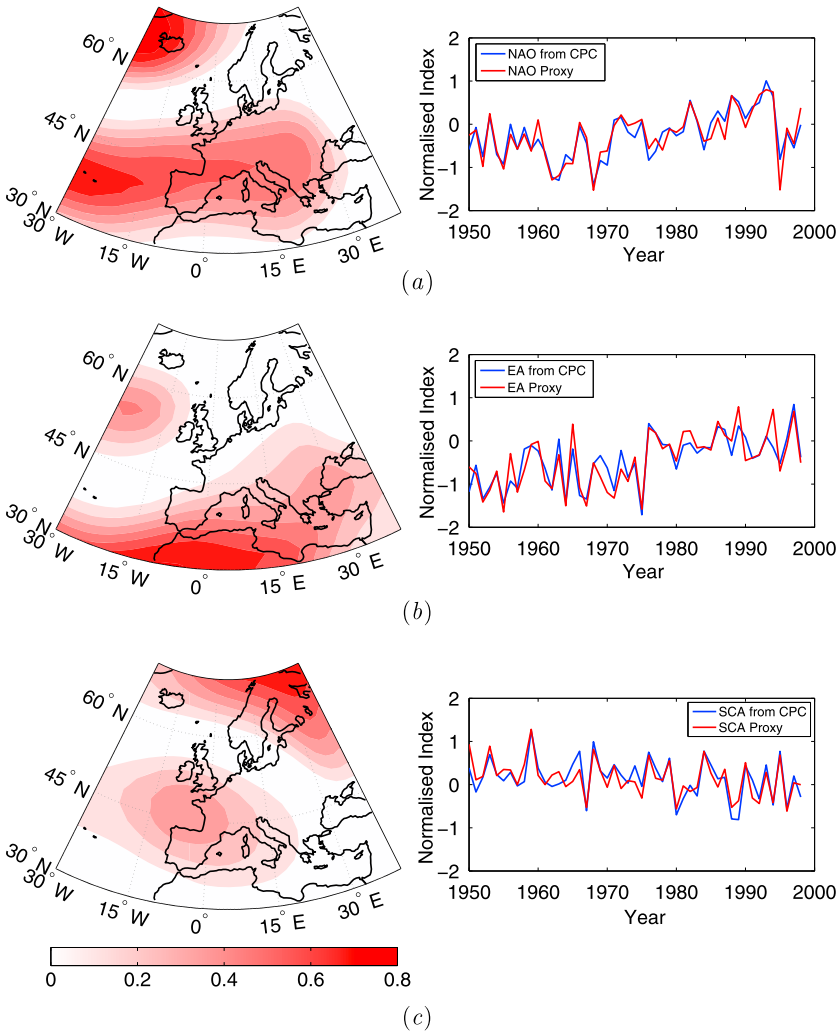

Figure 3. Spatial correlation of the monthly 500 mbar pressure fields from *Luterbacher et al.* [2002] against the known index (from Climate Prediction Center) and the comparison of the known index and the proxy index. (a) For the NAO. (b) For the EA. (c) For the SCA.

winter monthly pressure fields against the known indices of the NAO, the EA, and the SCA. The two regions of high color density show high correlation (R^2 = 0.4–0.8) with the known indices, which suggests a proxy based on the monthly pressure fields for each of the indices could be constructed. The spatial correlations of the three modes are in good agreement with the patterns identified by *Barnston and Livezey* [1987]. We note, however, that our regions of high correlation for the EA and the SCA do not lie on the same locations as the results from *Moore et al.* [2013] who conducted the full EOF analysis. This could be due to the finite size of sample for the analysis (50 years of data) and might also be due to rotation of the EOFs as well as the use of 6 month winter rather than a 3 month winter, as there is considerable variability in the locations of the centers of the action on a month-to-month basis [*Moore et al.*, 2013]. The proxy index for each of the teleconnection modes was then constructed by averaging by weight the pressure time histories of several points in the two regions of high correlation. Figure 3 (right column) shows the comparison of the known indices and proxy indices for the three signals during the period when the known indices and the pressure fields are available, and reasonable agreement is achieved with $R^2 > 0.7$.

The predictor model now uses the proxy indices for the three EOF modes and the comparison with the hindcast wave power. The correlation is still high for both Schiehallion and Haltenbanken, with $R^2 > 0.8$ (curiously slightly higher for the proxy indices than for the known indices), while the correlation for Forties for the total signal remains weaker with $R^2 = 0.44$ (see Figures S12 and S13 and Table S2 in the supporting information).

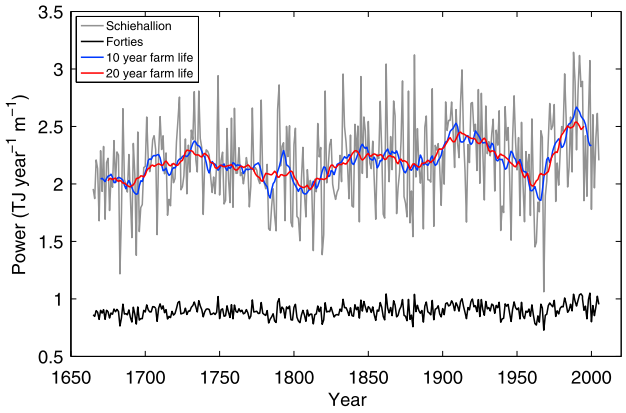

Figure 4. Reconstructed wave power for Schiehallion and Forties from 1665 to 2005. The predictor model uses proxy indices from 1665 to 1957 and known indices from 1957 to 2005.

Having trained the predictor model over the period of hindcast data, the model is back extrapolated to yield a representation of the historic wave power climate from 1665 to 2005, which consists of a combination of proxy indices from 1665 to 1957, and known indices from 1957 to 2005. The record is shown in Figure 4 for Schiehallion and Forties. A high level of interannual and multidecadal variability on all time scales at Schiehallion is observed: overall minimum to maximum differs by a factor of 3, and year to year fluctuates by a factor of 2. The decadal and longer scales of the variability will be obscured if the wave climate is assessed over a short period, for instance from 1960s to 1990s where the sea surface was observed to be getting rougher, while the long-scale analysis seems to imply that the increase in wave climate during that period was strongly influenced by the natural variability. The temporal variability at Forties is much smaller, indicating that this might be a better location for a wave power scheme — despite the lower long-term mean power available here.

The large-scale variability in Schiehallion has significant consequences on the viability of any wave energy converter farm. To assess the feasibility of a wave farm, a moving average was used to compute what the available average wave power resource over the life of a farm would have been depending on when the farm is built. On the same figure, 10 and 20 year moving averages are added, in which the interannual variability has been smeared out leaving only the long-term multidecadal fluctuation. Again, the result suggests considerable variation in the wave power output, which in this location indicates that the available wave power is an unreliable resource.

The reconstructed wave power climate shows consistent evidence with the occurrence of Little Ice Age, conventionally defined from the sixteenth to the nineteenth centuries [*Lamb*, 2002]. We observe nadirs for the coldest winters (when the NAO is in a negative mode leaving Northern Europe cold and dry) and peaks for the mildest winters (when the NAO is in a positive mode causing warm and wet) for instance from the average temperatures over December, January, and February in central England between 1659 and 1979 as documented in *Lamb* [2002]. Thus, only very low wave power may be available in the coldest winters when needed most. This consistency with the past evidence lends some support to the use of a proxy index based on reconstructed pressure fields.

Our reconstructed record clearly depends crucially on the reliability of the pressure maps reconstructed by *Luterbacher et al.* [2002]. Looking at the reconstructed record more closely, however, there seems to be more short-term variability after 1850 than before. The decrease in the short-term variability pre-1850 could be due to the fact that Luterbacher's earlier data were generally based on terrestrial observations (tree rings, ice cores, etc.) located in continental Eurasia which represent the marine regions less well [*Küttel et al.*, 2010], and only from nineteenth century onward data well into the Atlantic were included (Iceland from 1821, and the Azores and Madeira from 1865). Hence, one potential error is that the early period in Luterbacher's reconstruction could be more biased toward terrestrial observations. Incorporating more information from the open ocean such as wind information from ship log data could be useful to improve the reconstruction pre-nineteenth century. Also, both our linear model and the Luterbacher's reconstructed pressure fields assume stationarity over time in the relationship between the climate indices and the local wind and wave fields, and this could be another possible source of error [*Woollings et al.*, 2014].

The same correlation, partitioning, and reconstruction method have also been successfully applied to annual mean H_s, T_p, and T_m with comparable R^2 value (see Figures S14 and S15 in the supporting information). The reconstructed H_s record is helpful to identify any significant long-term trend, as some studies have claimed a global increasing trend in wind speeds and wave heights over the past two decades [see *Young et al.*, 2011, for example]. There does appear to be a weak long-term trend over the entire reconstruction period, but this

is much weaker than the decadal variability which has dominated in recent decades. Further discussion of this is given in the supporting information.

5. Conclusions

Annual mean wave power is very variable, particularly in the open North Atlantic. Good correlation is obtained between the wave power from hindcast data and the climate indices. This suggests most of the variability of the wave power is correlated to the interannual and multidecadal trend of the NAO and other modes. A simple method to obtain a set of proxy indices is introduced to extrapolate the wave climate back into the past. The historic wave climate record reveals high level of variability on all time scales for the locations in the open North Atlantic and much smaller variability for the location in the North Sea. In order to improve the predictability for the wave power production over decades into the future, it is essential to first understand and improve the forecasting of the NAO into the future. The recent results of *Smith et al.* [2014] are encouraging in this regard.

Acknowledgments

We thank Richard Gibson at BP Sunbury for providing the wave data and acknowledge support from EPSRC (project EP/J010316/1 Supergen MARine TechnologY challenge). The climate indices are available from the NOAA/CPC (ftp://ftp.cpc.ncep.noaa.gov/wd52dg/data/indices/tele_index.nh). The reconstructed 500 mbar pressure maps by *Luterbacher et al.* [2002] are available at https://www.ncdc.noaa.gov/paleo/pubs/luterbacher2002/luterbacher2002.html. Please contact the corresponding author for the proxy indices.

The Editor thanks two anonymous reviewers for their assistance in evaluating this paper.

References

Allan, J., and P. Komar (2000), Are ocean wave heights increasing in the eastern North Pacific?, *Eos Trans. AGU*, *81*(47), 561–567.

Bacon, S., and D. Carter (1991), Wave climate changes in the North Atlantic and North Sea, *Int. J. Climatol.*, *11*(5), 545–558.

Bacon, S., and D. Carter (1993), A connection between mean wave height and atmospheric pressure gradient in the North Atlantic, *Int. J. Climatol.*, *13*(4), 423–436.

Barnston, A. G., and R. E. Livezey (1987), Classification, seasonality and persistence of low-frequency atmospheric circulation patterns, *Mon. Weather Rev.*, *115*(6), 1083–1126.

Carter, D., and L. Draper (1988), Has the north-east Atlantic become rougher?, *Nature*, *332*, 494.

Cassou, C., M. Minvielle, L. Terray, and C. Périgaud (2011), A statistical-dynamical scheme for reconstructing ocean forcing in the Atlantic. Part I: Weather regimes as predictors for ocean surface variables, *Clim. Dyn.*, *36*(1–2), 19–39.

Group, T. W. (1988), The WAM model—A third generation ocean wave prediction model, *J. Phys. Oceanogr.*, *18*(12), 1775–1810.

Hurrell, J. W. (1995), Decadal trends in the North Atlantic Oscillation: Regional temperatures and precipitation, *Science*, *269*(5224), 676–679.

Hurrell, J. W., and H. Van Loon (1997), Decadal variations in climate associated with the North Atlantic Oscillation, in *Climatic Change at High Elevation Sites*, pp. 69–94, Springer, Dordrecht, Netherlands.

Hurrell, J. W., Y. Kushnir, G. Ottersen, and M. Visbeck (2003), *An Overview of the North Atlantic Oscillation*, AGU, Washington, D. C.

Kushnir, Y., V. Cardone, J. Greenwood, and M. Cane (1997), The recent increase in North Atlantic wave heights, *J. Clim.*, *10*(8), 2107–2113.

Küttel, M., E. Xoplaki, D. Gallego, J. Luterbacher, R. Garcia-Herrera, R. Allan, M. Barriendos, P. Jones, D. Wheeler, and H. Wanner (2010), The importance of ship log data: Reconstructing North Atlantic, European and Mediterranean sea level pressure fields back to 1750, *Clim. Dyn.*, *34*(7–8), 1115–1128.

Lamb, H. H. (2002), *Climate, History and the Modern World*, Routledge, London.

Luterbacher, J., E. Xoplaki, D. Dietrich, R. Rickli, J. Jacobeit, C. Beck, D. Gyalistras, C. Schmutz, and H. Wanner (2002), Reconstruction of sea level pressure fields over the Eastern North Atlantic and Europe back to 1500, *Clim. Dyn.*, *18*(7), 545–561.

Mackay, E. B., A. S. Bahaj, and P. G. Challenor (2010), Uncertainty in wave energy resource assessment. Part 2: Variability and predictability, *Renewable Energy*, *35*(8), 1809–1819.

Moore, G., I. Renfrew, and R. S. Pickart (2013), Multidecadal mobility of the North Atlantic Oscillation, *J. Clim.*, *26*(8), 2453–2466.

Neill, S. P., and M. R. Hashemi (2013), Wave power variability over the northwest European shelf seas, *Appl. Energy*, *106*, 31–46.

Neill, S. P., M. J. Lewis, M. R. Hashemi, E. Slater, J. Lawrence, and S. A. Spall (2014), Inter-annual and inter-seasonal variability of the Orkney wave power resource, *Appl. Energy*, *132*, 339–348.

Reistad, M., Ø. Breivik, H. Haakenstad, O. J. Aarnes, B. R. Furevik, and J.-R. Bidlot (2011), A high-resolution hindcast of wind and waves for the North Sea, the Norwegian Sea, and the Barents Sea, *J. Geophys. Res.*, *116*, C05019, doi:10.1029/2010JC006402.

Shimura, T., N. Mori, and H. Mase (2013), Ocean waves and teleconnection patterns in the northern hemisphere, *J. Clim.*, *26*(21), 8654–8670.

Smith, D. M., A. A. Scaife, R. Eade, and J. R. Knight (2014), Seasonal to decadal prediction of the winter North Atlantic Oscillation: Emerging capability and future prospects, *Q. J. R. Meteorol. Soc.*, doi:10.1002/qj.2479.

Tucker, M. J., and E. G. Pitt (2001), *Waves in Ocean Engineering*, vol. 5, Elsevier, Amsterdam.

Unden, P., et al. (2002), HIRLAM-5 scientific documentation.

Uppala, S. M., et al. (2005), The ERA-40 re-analysis, *Q. J. R. Meteorol. Soc.*, *131*(612), 2961–3012.

Wentz, F. J., L. Ricciardulli, K. Hilburn, and C. Mears (2007), How much more rain will global warming bring?, *Science*, *317*(5835), 233–235.

Woolf, D. K., P. Challenor, and P. Cotton (2002), Variability and predictability of the North Atlantic wave climate, *J. Geophys. Res.*, *107*(C10), 3145, doi:10.1029/2001JC001124.

Woollings, T., A. Hannachi, and B. Hoskins (2010), Variability of the North Atlantic eddy-driven jet stream, *Q. J. R. Meteorol. Soc.*, *136*(649), 856–868.

Woollings, T., C. Franzke, D. Hodson, B. Dong, E. Barnes, C. Raible, and J. Pinto (2014), Contrasting interannual and multidecadal NAO variability, *Clim. Dyn.*, *45*, 539–556.

Young, I., S. Zieger, and A. Babanin (2011), Global trends in wind speed and wave height, *Science*, *332*(6028), 451–455.

Young, I., J. Vinoth, S. Zieger, and A. Babanin (2012), Investigation of trends in extreme value wave height and wind speed, *J. Geophys. Res.*, *117*, C00J06, doi:10.1029/2011JC007753.

Zieger, S., A. Babanin, and I. Young (2014), Changes in ocean surface wind with a focus on trends in regional and monthly mean values, *Deep Sea Res., Part I*, *86*, 56–67.